Current Opinion in Solid State and Materials Science 16 (2012) 82–90

Contents lists available at SciVerse ScienceDirect

Current Opinion in Solid State and Materials Science

journal homepage: www.elsevier.com/locate/cossms

Applications of optomechanical effects for on-chip manipulation of light signals

Jing Ma, Michelle L. Povinelli *

Ming Hsieh Department of Electrical Engineering, 3737 Watt Way, PHE 614, Los Angeles, CA 90089-0271, USA

ARTICLE INFO

Article history:
Received 2 August 2011
Accepted 6 December 2011
Available online 23 December 2011

Keywords:
Nanophotonics
Optomechanics
Optical forces
Photonic crystals
Microresonators
Integrated photonics

ABSTRACT

We review recent developments in the study of optical forces in integrated photonics. Our initial predictions suggested that freely suspended, parallel silicon waveguides should exhibit significant forces due to mode coupling. Symmetric and anti-symmetric modes give rise to attractive and repulsive modes respectively, analogous to bonding and anti-bonding orbitals in solid state physics. Experimental demonstrations of forces in waveguide and microresonator systems rapidly followed. We review recent work on applications of optical forces to on-chip manipulation of light signals.

1. Introduction

It has long been known that light can exert a force on objects, an effect known as radiation pressure. One well-known application of optical forces is optical trapping [1,2], a technique that uses laser light to manipulate nanoscale objects. In the optics field, the force of light on the parallel mirrors making up a Fabry–Perot cavity has been studied for both classical [3] and quantum–mechanical applications [4,5].

Our work [6] has introduced the idea of using optical forces to precisely control the positions of microscale optical waveguides and resonators. Optical waveguides, which act like "photonic wires," and microresonators, devices that confine light to the scale of the wavelength, are important elements for developing photonic integrated circuits [7–11]. Ultimately, photonic integrated circuits may manipulate photons the way that electronic circuits manipulate electrons. The development of photonic circuits that can filter, buffer, and reroute optical signals is expected to transform optical communications [12], enable high-speed optical interconnects between multi-chip computer processors [12–16], and provide a platform for quantum communication [17]. However, current photonic circuits are largely static; methods for reconfiguring their response are limited. Optical forces in integrated photonics, or *optomechanical effects*, represent an exciting new approach for achieving flexible, all-optical tuning and reconfiguration of on-chip microphotonic devices.

In Section 2, we review the basic physics of the optical force between waveguides and microresonators. We briefly review the early experiments that demonstrated motion due to optical forces in integrated microphotonic systems. In Section 3, we outline the calculation methods for accurately determining optical forces in realistic structures. In Section 4, we review a range of microphotonic device geometries that exhibit strong optomechanical effects. In Section 5, we summarize recent work on applications of optical forces to on-chip manipulation of optical signals such as switching, filtering, and buffering of signals. Lastly, in Section 6, we conclude with opportunities and challenges for future work.

For the purposes of this review, we assume familiarity with basic concepts and device structures of micro- and nanophotonics, in particular photonic crystals [18] and microresonators [19]. We focus on applications of optomechanics to the control and repositioning of on-chip, integrated microphotonic devices. Other fascinating aspects of optomechanics, such as optomechanical ground-state cooling and associated quantum phenomena, are covered elsewhere [20–22].

2. Optical forces: basic effect and early experiments

In 2005, Povinelli et al. theoretically investigated the optical forces between parallel waveguides [6], shown in Fig. 1a. We showed that a mechanical force arises from the overlap of the guided waves propagating in the two waveguides. The sign of the force can be either attractive or repulsive, depending on the relative phase of light in the waveguides. The "bonding" mode, which is symmetric with respect to the two waveguides, gives an attractive optical force, whereas the "anti-bonding," or anti-symmetric mode, is repulsive. By controlling which mode is input into the waveguides, input light can be used to pull the waveguides together or push them apart. Physically, the force originates from

* Corresponding author.
E-mail address: povinell@usc.edu (M.L. Povinelli).

1359-0286/$ - see front matter © 2011 Elsevier Ltd. All rights reserved.
doi:10.1016/j.cossms.2011.12.001

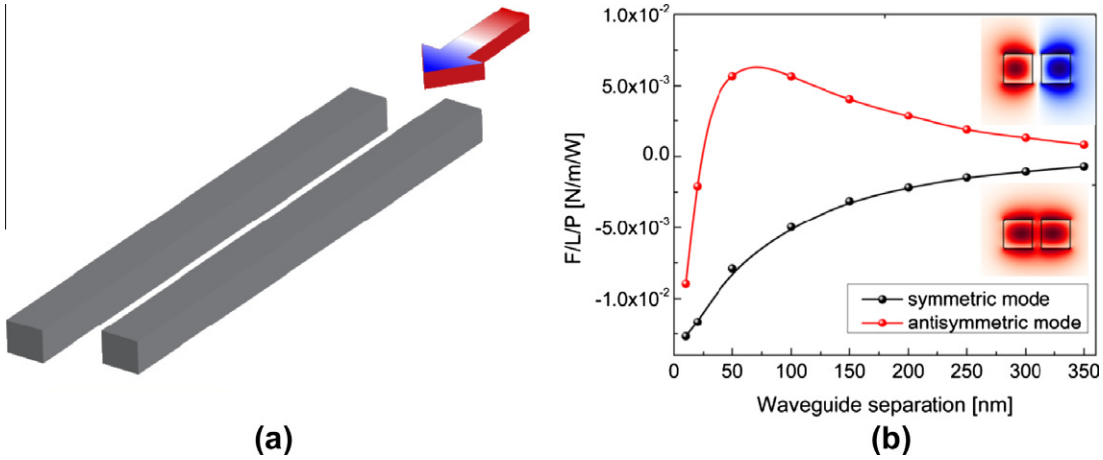

Fig. 1. Optical forces between parallel waveguides. (a) Schematic structure; multicolored arrow indicates the direction of light propagation. (b) Calculated, normalized, optical force as a function of waveguide separation. Insets show modal profiles, with red/blue indicating positive/negative values of the electric field component parallel to the air gap.

the interaction of dipoles induced in the dielectric waveguides by the electromagnetic field of the light wave. The optical force scales linearly with input power.

The calculated optical force in a typical system is shown in Fig. 1b. The waveguides each have cross sections of 310 nm by 310 nm, and the wavelength in air is 1550 nm. In the figure, the force per unit length of the waveguide is divided by the input power and plotted as a function of waveguide separation. For waveguide separations larger than ~60 nm, the symmetric and antisymmetric modes correspond to attractive (positive sign) and repulsive (negative sign) forces, respectively. The magnitude of the optical force decays monotonically with increasing separation. The decay is due to reduced optical coupling between the waveguides, that is, reduced overlap between the evanescent tails of the individual waveguide modes. For smaller waveguide separations, strong coupling between the waveguides can significantly perturb the individual waveguide modes. In this regime, the optical force of the antisymmetric mode changes sign.

From Fig. 1b, we can see that for the symmetric (attractive) mode, the optical force increases with decreasing gap. However, if the gap is too small, the Casimir force becomes comparable to, or larger than, the optical force [23]. Devices with gaps as small as ~80 nm have been used in experiments [24].

Interestingly, the optical force between waveguides is in a direction parallel to the direction of light propagation. This is different than the traditional case of radiation pressure, where the optical force on a surface is parallel to the direction of light propagation. The radiation pressure can be simply derived from momentum conservation arguments: reflection of a photon from a surface must correspond to transfer of mechanical momentum to the surface. Similarly, the optical force on the mirrors of a Fabry–Perot cavity acts perpendicular to the direction of light propagation [3]. For parallel waveguides, the situation is notably different: the momentum acquired by each individual waveguide is perpendicular to the propagation direction, and the momenta of the two waveguides are equal and opposite.

Theoretical work by ourselves and other authors predicted optical forces in other waveguide structures [25,26], coupled microphotonic resonators [27,28], and double-layer photonic crystal slab cavities [29]. For two closely-positioned resonators, coupling between the resonant modes can yield attractive or repulsive forces in a similar way to parallel waveguides.

Initial theoretical work on optical forces was followed rapidly by experimental demonstrations. Van Thourhout and Roels [30] have written a recent comprehensive review.

In 2008, a suspended waveguide coupled to an underlying substrate was designed [31] and fabricated [32] by Li et al. A schematic is shown in Fig. 2a. The authors demonstrated an attractive optical force that is induced by the overlap between the evanescent tail of waveguide mode and the underlying oxide substrate. Waveguide displacement was inferred from the optical transmission using an on-chip interferometer scheme. Further experiments demonstrated attractive and repulsive forces in coupled microresonators, shown in Fig. 2b. Rosenberg et al. [33] and Wiederhecker et al. [34] measured attractive and repulsive optical forces in vertically-stacked microdisk resonator systems.

3. Methods for calculation of optical forces

Accurate calculations of optical forces in realistic, 3D structures can be performed using electromagnetic modeling techniques.

One method for force calculation is to evaluate the Maxwell stress tensor (MST) numerically [35]. This general, flexible technique allows one to directly calculate the force based on the full electromagnetic field distributions, which can be obtained from an appropriate full-vectorial electromagnetic solver. The MST method has been used to evaluate optical forces in many contexts [25,29,36–38]. To compute the optical forces acting on a movable component, the Maxwell stress tensor is numerically integrated over a closed surface surrounding the component:

$$\mathbf{F}_\alpha = \oint_s \sum_\beta T_{\alpha\beta} n_\beta da, \tag{1}$$

where α and β indicate direction x, y or z, $\mathbf{n}$ is the outward normal to the closed surface S, and the stress tensor,

$$T_{\alpha\beta} = \varepsilon E_\alpha E_\beta + \mu H_\alpha H_\beta - \frac{1}{2}\delta_{\alpha\beta}(\varepsilon \mathbf{E}\cdot\mathbf{E} + \mu \mathbf{H}\cdot\mathbf{H}).$$

Typically, the time scale for mechanical response is longer than the optical period, and the time-averaged force over the optical period may be considered [38]. The disadvantage of the MST method is that since it requires the knowledge of the full electromagnetic fields, it is computationally intensive and can become prohibitive for large system size.

We have shown previously [6] that for infinitely long waveguides with no radiation loss, the force between two waveguides can be calculated from the derivative of the eigenmode frequency with respect to separation. This relationship follows from express-

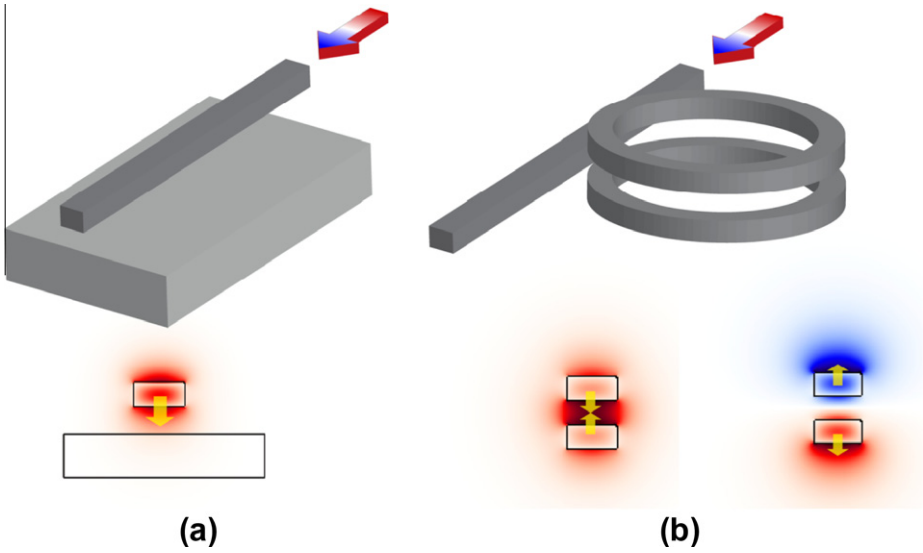

Fig. 2. Optical forces (a) between waveguide and substrate, and (b) between vertically-stacked microrings. Light is coupled into the rings by a bus waveguide. For both (a) and (b), the structure is shown on top, with a multicolored arrow labeling the direction of light propagation. The modal profiles are shown on the bottom, with red/blue indicating positive/negative values of the electric field component perpendicular to the air gap. Yellow arrows show the direction of the optical force. The system in (a) has an attractive mode only, whereas (b) has both symmetric (attractive) and anti-symmetric (repulsive) modes.

ing the force as a derivative of the electromagnetic energy U with respect to waveguide separation, g:

$$F = -\frac{dU}{dg}\bigg|_k = -\frac{d(Nh\omega)}{dg}\bigg|_k = -Nh\frac{d\omega}{dg}\bigg|_k = -\frac{U}{\omega}\frac{d\omega}{dg}\bigg|_k, \tag{2}$$

where N is the number of photons, ω is the eigenmode frequency, and k is the wave vector.

An optomechanical coupling constant can be defined as $g_{OM} = d\omega/dg$. The value of g_{OM} is proportional to the force per photon (F/N) on the mechanical system. Larger values of g_{OM} indicate a larger change in the optical properties of the system for a given mechanical displacement.

It is often convenient to consider the force per unit length of the waveguide, normalized to the input power P. Under conditions of fixed power input to a guided-wave mode, the electromagnetic field energy U scales as the input power over the group velocity: $U = PL/v_g$. The normalized force is:

$$\frac{F}{PL} = -\frac{1}{v_g\omega}\frac{d\omega}{dg}\bigg|_k, \tag{3}$$

Consequently, reducing the group velocity of a mode tends to increase the optical force per unit waveguide length at fixed input power. The force may alternately be written as a derivative of the effective index n_{eff} with respect to separation [31]:

$$\frac{F}{PL} = \frac{1}{v_g n_{\text{eff}}}\frac{dn_{\text{eff}}}{dg}\bigg|_k, \tag{4}$$

In Eqs. (3) and (4), the derivatives are taken at fixed wave vector. The derivative can be alternately be recast at fixed frequency [39]:

$$\frac{F}{PL} = \frac{1}{c}\frac{dn_{\text{eff}}}{dg}\bigg|_\omega, \tag{5}$$

Derivative methods generally assume that the optomechanical system is closed and does not exchange energy with the surrounding media. The force between two microcavities can also be calculated as a derivative of the cavity mode frequency with respect to separation, provided that the cavity quality factor is large [27,29]. For microresonator systems, the optical force is proportional to the electromagnetic field energy stored in the resonators.

Rakich et al. have shown that for general linear, lossless systems, the force can be written in terms of the scattering matrix [40]. This method is particularly useful for systems that can be accurately described by coupled-mode theory [41], such as systems of multiple microresonators coupled to waveguides, in which full-field calculations can prove prohibitive.

Given the value of the optical force at a given optical power level, a resulting static displacement can be calculated by solving the corresponding mechanical problem. A typical approach is to use finite element software, such as COMSOL, for this purpose.

4. Microphotonic device geometries exhibiting strong optomechanical effects

Following initial work on waveguide and microresonator systems, a variety of alternate microphotonic device geometries have been investigated. Various mechanisms have been studied for enhancing the optical force. These include tailoring the overlap between photonic and mechanical modes, exploiting guided resonance modes, reducing the group velocity of propagating light, and incorporating plasmonic materials. Below, we review work on these interesting microphotonic device concepts.

4.1. Microcavity systems

Photonic-crystal microcavities can be designed to confine light in ultra-small mode volumes and exhibit high optical quality factors, Q [42–45]. Recent work has exploited these attributes to achieve strong optomechanical effects.

Chan et al. [46] and Eichenfield et al. [47] have designed and experimentally demonstrated a "zipper" system with large optomechanical coupling. The zipper is made up of two parallel, patterned nanobeams (shown in Fig. 3a) each of which is designed to support an optical microcavity mode. Coupling between the modes gives rise to attractive and repulsive forces. A relevant figure of merit in the structure is the optomechanical coupling length, $L_{OM} = \omega/g_{OM}$, where ω is the optical resonance frequency. Experimental values lower than 3 μm were obtained.

In this system, optomechanical coupling results in an "optical spring effect:" due to the presence of optical forces, the mechanical resonance frequency and spring constant are shifted. In experiments, a modified stiffness of five times the intrinsic mechanical stiffness of the nanobeam was observed.

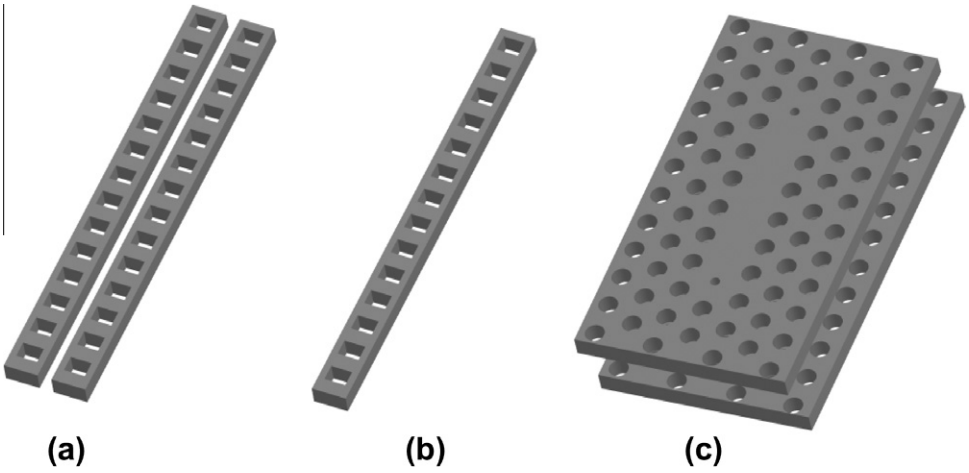

Fig. 3. Schematic of photonic crystal cavities showing opto-mechanical coupling. (a) "zipper" cavity, (b) nanobeam cavity, and (c) double-layer photonic crystal slab cavities. In (a) and (b), the lattice constant near the center of the device is decreased slightly (not shown) to form a microcavity.

In Ref. [48], Painter and co-workers designed and experimentally demonstrated a nanobeam structure (in Fig. 3b) that confines *both* the optical modes and the mechanical vibration modes to the scale of the optical wavelength. Localized mechanical modes are created using a *phononic* band gap microcavity, analogous to the optical case. The authors suggest that the strong optomechanical coupling between optical modes (200 THz optical resonance frequency) and high-frequency mechanical modes (2 GHz mechanical resonance frequency) will allow extremely sensitive mass detection via optical readout.

Notomi and coworkers have theoretically analyzed microcavities in parallel photonic-crystal slabs [29]. A schematic double-layer cavity is shown in Fig. 3c. Intriguingly, the authors suggest that if the mechanical displacement between the structures occurs faster than the response time of the optical cavity (proportional to the optical period times the optical Q), wavelength conversion will occur [49]. This phenomenon is analogous to the frequency shifts predicted and measured in microphotonic systems with time-varying linear refractive index [50,51].

4.2. Guided resonance systems

When light is normally incident upon a 1D- or 2D-periodically patterned slab, it can excite *guided resonance modes*, which propagate in the plane of the slab while leaking partially to the surrounding air [52]. Early work examined forces between identical, parallel photonic-crystal slabs (Fig. 4a). Liu et al. [53] showed theoretically that optical forces are enhanced near guided resonances. In an ideal system, infinite-Q resonances, or "dark states" can be designed, and the force will diverge as $1/Q$ near the resonant frequency. Experiments on a similar system were reported by Roh et al. [54]. Changes in separation between the slabs due to optical forces were inferred from the optical reflection spectrum. Displacements of approximately 3.6 nm were obtained for $\sim$20 mW of power. The force per photon, 0.051 pN/photon, was similar to values obtained in double-layer disk cavities [33] and zipper cavities [47].

Rodriguez et al. [55] have theoretically studied asymmetric systems consisting of a photonic-crystal slab above an unpatterned, layered substrate, shown in Fig. 4b. This system may offer advantages in terms of fabrication. The asymmetric system supports both quasi-symmetric and quasi-antisymmetric modes with opposite signs of the force. As for symmetric structures, the sign of the force can be changed by tuning the frequency of the incident light. Assuming the photonic-crystal slab can move, changing the separation between slab and substrate, bistable behavior is predicted [56]. The precise conditions for bistability are affected by the Casimir force, suggesting that observations of bistability could be used to infer the magnitude of the Casmir force. In addition, the optical

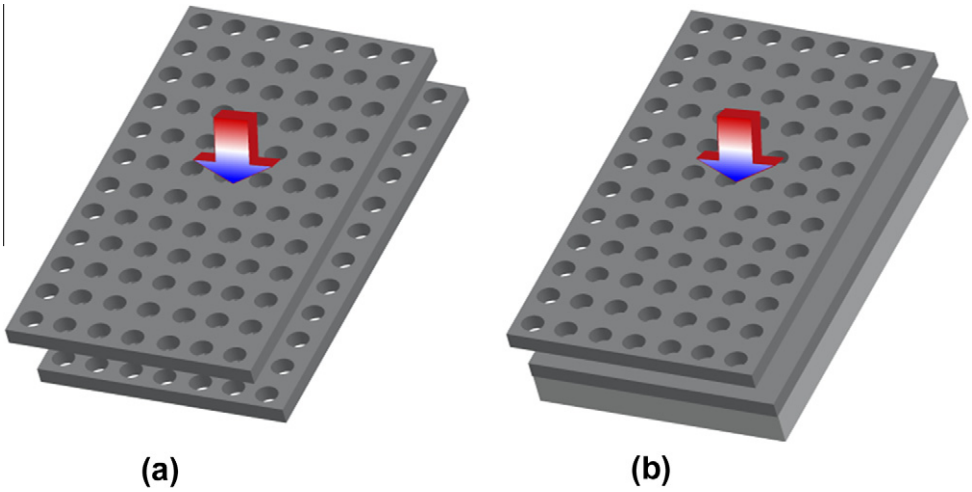

Fig. 4. Guided-resonance optomechanical devices: (a) double-layer photonic crystal slab supporting guided resonances, and (b) asymmetric guided resonant structure composed of photonic crystal slab and silicon–silica substrate.

force might be used as a way of controlling or preventing stiction, which results from Casimir attraction.

One advantage of such guided-resonant devices is that light can be coupled into the mode at normal incidence using free-space optics, potentially allowing ease of alignment. However, the mass of guided-resonant slabs is usually bigger than that of photonic crystal cavity devices, which may reduce the mechanical resonance frequency and hence increase the characteristic response time for an optical force.

4.3. Slow-light enhanced systems

A variety of microphotonic devices support propagating modes with slow light speeds. Povinelli et al. have examined the effect of slow light on optical force enhancement [36]. The system considered is shown in Fig. 5a. Light propagates in the air gap between the two films, pushing them apart. The optical force is proportional to the light intensity in the propagating mode. Under conditions of fixed power input to a guided-wave mode, the light intensity scales as the input power over the group velocity (see Eq. (3)). Consequently, reducing the group velocity of a mode increases the optical force for fixed input power. In the extreme case, as the light group velocity approaches zero, the optical force diverges.

The slow-light enhancement mechanism is not unique to the particular waveguide structure in Ref. [36]. In Ref. [57], we calculated the forces between a suspended, one-dimensionally periodic photonic-crystal waveguide and an underlying substrate, as shown in Fig. 5b. For constant wavelength, the force is enhanced when the waveguide-substrate separation is adjusted to tune the propagating mode close to cutoff. Moreover, the force is non-monotonic as a function of increasing separation.

The main challenges for slow-light enhancement are input coupling and scattering losses. To efficiently inject power into a slow-light mode, input tapering strategies are generally required [58,59]. Moreover, the increase in scattering loss with decreasing group velocity [60–62] will limit the achievable enhancement factors.

4.4. Plasmonic systems

Surface Plasmon Polaritons (SPP's) are propagating electromagnetic modes formed at metallic-dielectric interfaces [63] that offer the ability to confine light to the deep subwavelength scale. There has been interest in determining whether the enhanced light intensity can be exploited to yield large optical forces. Woolf et al. [64] have theoretically analyzed the forces generated by SPP's between metal slabs. They determined that semi-infinite metal waveguides separated by an air gap (MIM geometry as shown by Fig. 6a) give rise to an attractive force, while finite-thickness metal waveguides separated by an air gap (IMIMI geometry as shown by Fig. 6b) yield either attractive or repulsive forces, depending on the mode. The authors focus consideration on modes with long-range propagation characteristics, for which the field overlap with the metal, and consequently the loss, is relatively low.

Two papers have calculated force enhancements in hybrid plasmonic waveguides consisting of dielectric waveguides coupled to metallic substrates (Fig. 6c). Refs. [65,66] show that the force between a silicon waveguide and a metal substrate is up to an order of magnitude larger than the force between the same waveguide and a dielectric substrate, given the same cross-sectional power. However, this conclusion applies only for relatively small waveguide-substrate gaps. The plasmonic enhancement is non-resonant, and thus can be used for a broad range of wavelengths. However, due to ohmic loss, the hybrid plasmonic mode decays in the propagation direction. As a result, the enhancement will only be maintained for distances shorter than the plasmon decay length, typically on the order of 10's of microns.

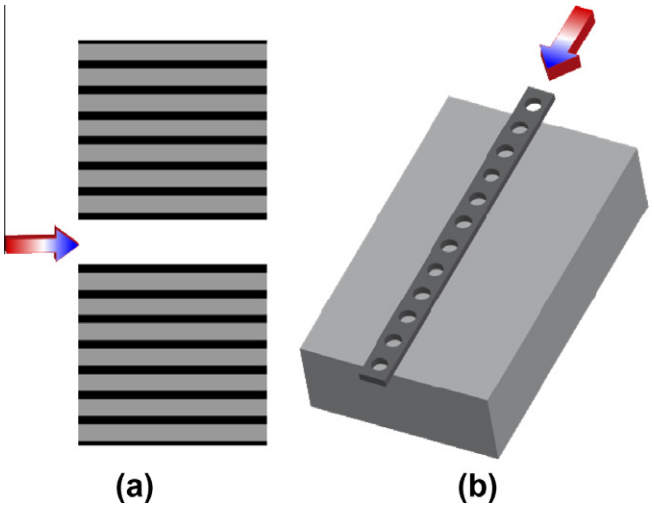

Fig. 5. Devices that enhance optomechanical effects via slow light: (a) waveguide formed by reflective multilayer films, (b) one-dimensionally periodic photonic crystal waveguide coupled with silica substrate.

5. Applications of on-chip information processing

As discussed above, optical forces have been calculated for a range of microphotonic device geometries, and mechanical motion arising from optical forces has been measured in a variety of experiments. In this section, we will discuss some of the applications of these effects in on-chip information processing, such as filtering, switching, and other operations.

Optomechanical techniques offer particular advantages and disadvantages relative to other methods for tuning the response of a microphotonic system. Mechanical motion results in a large change in the effective index of a microphotonic structure, as compared to other tuning mechanisms such as thermal, electrooptic, and carrier injection. Thermal tuning through 10 K, for example, changes the index of silicon by less than 0.07%. Mechanical motion changes the refractive index by order unity, due to the large index difference between silicon and air. The characteristic time scale for optomechanical effects is determined by the mechanical motion. If the device is operated in steady state, the time scale is determined by the mechanical period (proportional to the inverse mechanical resonance frequency). This number sets a lower limit on the time scale for response. If the optical signal is switched on abruptly, the mechanical displacement will equilibrate on a time scale determined by the product of the mechanical period and the mechanical quality factor.

With these general features in mind, we discuss how optomechanical effects can be used to construct novel, tunable, on-chip optical components. These include devices for nonlinear signal processing, optical power regulation, wavelength filtering, self-adaptive microcavities, slow-light effects, and tunable lasers.

5.1. Nonlinear signal processing

The essence of an optical nonlinearity is that the propagation characteristics of a device change with incident power. This is the case for optomechanical effects. Light results in a force that physically moves the device, affecting light propagation.

Pernice et al. [67] have examined the *mechanical Kerr nonlinearity* between a movable silicon waveguide and an underlying

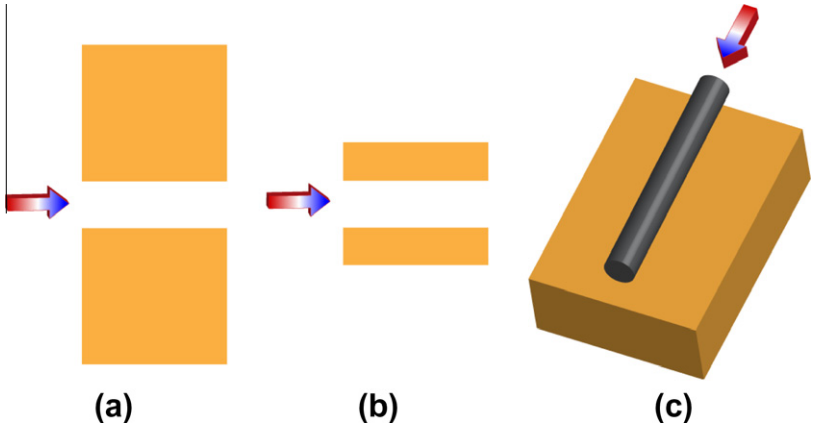

Fig. 6. Optical forces generated in plasmonic devices: (a) semi-infinite metal plates separated by an air gap, (b) finite-thickness metal waveguides separated by an air gap, and (c) a hybrid plasmonic system with a dielectric waveguide and a metallic substrate.

substrate. In such a system (Fig. 2a), light in the waveguide induces a force that attracts the waveguide to the substrate. The resulting motion changes the effective index of the waveguide mode. Because the optical force increases with intensity, the net effect is an intensity-dependent mode index that can be described by a mechanical Kerr coefficient. The mechanical Kerr coefficient is several orders of magnitude larger than the ordinary Kerr coefficient of silicon. We have studied the mechanical Kerr effect in coupled-waveguide systems (Fig. 1a), where the force between waveguides can be either attractive or repulsive [39]. We have shown that either sign of the force results in a positive, giant mechanical Kerr coefficient and shown how the magnitude can be optimized with appropriate device parameters.

We have also theoretically proposed that optomechanical effects could be used to achieve *all-optically tunable birefringence* [68]. We have analyzed birefringence in a system of two coupled waveguides (Fig. 1a). By tuning the pump power injected in the waveguide, the separation between the waveguides can be adjusted. The change in separation affects the relative phase between TE and TM polarized modes. For appropriate values of the pump power, the device acts as a polarization converter, changing linear to circularly polarized light.

The ability to achieve mechanical Kerr effects and optically-tunable polarization rotation suggest that optomechanical effects can be used in a variety of switching configurations. The use of non-resonant devices should allow wide bandwidth response.

5.2. Tunable directional coupler

One example of a waveguide switch is a directional coupler [69]. The standard directional coupler design consists of two parallel waveguides. Light input to one waveguide transfers to the other waveguide over a characteristic length scale called the coupling length. For proper adjustment of the device length, L, all input light is transferred to the drop port. Tuning the effective index of the waveguides changes the coupling length, also changing the fraction of power that is output at the through and drop ports.

Fong et al. [70] have used optical forces to demonstrate an all-optically tunable directional coupler. Each of the waveguides is a slot waveguide (Fig. 7). An optical pump signal is used to induce an optical force, which reduces the slot width. The change in slot width causes a change in effective index of each slot waveguide, changing the behavior of the coupler. The authors demonstrated that the output power of a probe signal at the drop port could be tuned from 0.1% to 70% using 1.3 mW pump power. Dynamic modulation was also demonstrated.

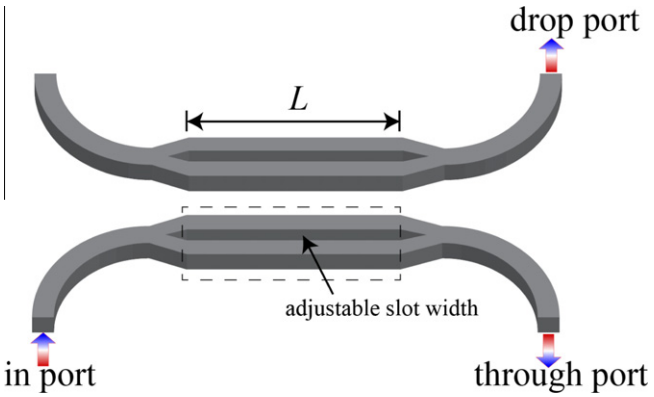

Fig. 7. Optically-tunable directional coupler, in which the effective index of each arm is tuned via an adjustable slot width. Figure adapted from [70].

5.3. Optical power regulation

Optomechanical response also offers the opportunity to control or regulate transmitted power levels. In Ref. [57], we have calculated optical forces between a periodically-patterned, movable silicon waveguide and a substrate (Fig. 5b). For a given wavelength of operation, the separation between waveguide and substrate will determine whether light propagates or falls in the photonic bandgap of the device. For proper design, increasing the optical power will pull the waveguide toward the substrate, moving the waveguide into the bandgap and prohibiting propagation. This effect should limit the total amount of power that can be transmitted through the device.

The design of novel devices that perform the reverse function, only allowing transmission above certain power levels, will allow the regulation of power levels on chip. In combination with gain elements, optomechanical elements could thus provide a way to adaptively shape the average power of signal bit streams.

5.4. Wavelength filtering

Optical forces provide a method to achieve wideband tuning of microcavity resonances, with potential applications to filtering and routing.

In an early paper, Eichenfield et al. [71] demonstrated an all-optical tunable filter based on a high-Q silicon nitride microresonator coupled to a movable silica waveguide. The optical force due to a strong pump beam pulls the waveguide toward the

microresonator, changing the resonance frequency at a probe wavelength. The pump wavelength was tuned to change the waveguide-resonator separation, shifting the probe transmission spectrum.

Two papers have demonstrated tunable filters based on power tuning of a pump beam. Conceptually, the devices used are similar to Fig. 2b; stacked microrings support coupled optical modes. The rings are mechanically supported by hub-and-spoke structures (not shown), which can be tailored to control the effective spring constant of the mechanical modes.

Rosenberg et al. [33] demonstrated the use of optical forces to tune the microcavity resonance in a double-ring, silica "spiderweb" structure. The optical force changes the separation between the rings, shifting the resonance. Static tuning was demonstrated with an efficiency of 2.5 nm/mW. Dynamic tuning was demonstrated with a switching time less than 200 ns.

Wiederhecker et al. [72] later used optical forces to tune the optical resonance of a silicon nitride "double wheel" microcavity. Tuning of 30 nm was achieved with an efficiency of 2.3 nm/mW. The authors argue that the tuning range is ultimately limited by the onset of mechanical regeneration.

In both these papers, the transmission line shape is a dip, or rejection filter. It has been suggested that modified devices and measurement configurations could be used to demonstrate related functions, such as routing, switching, buffering, dispersion compensation, pulse trapping and release, and tunable lasing [33]. The wide tunability suggests these functions could be achieved over the full telecom C- or L-bands [72].

5.5. Self-adaptive microcavity

Rakich et al. [28] have proposed theoretically that optical forces can be used to design self-adaptive microcavities, cavities which tune themselves to the incident laser frequency. This behavior is achieved by careful design of the optomechanical potential in a modified, double-ring system, shown in Fig. 8. The waveguide on the right is used to couple light into the rings. The force between rings is attractive at large separations and repulsive at small ones. As a result, the ring separation will adjust to a stable, intermediate separation value. Using the optical forces between an additional pair of coupled waveguides (shown on the left) to further shape the optomechanical potential, the system can be designed so that the stable ring separation always corresponds to a resonance frequency equal to the incident laser frequency.

The concept of a self-aligning microcavity may provide a route to more robust on-chip microcavity devices [73]. Temperature variations, fabrication error, and other factors all influence the resonant frequencies of microcavities. Using optomechanical effects, a reference laser could be used to lock multiple microcavity devices on a chip (such as filters) to a standard frequency.

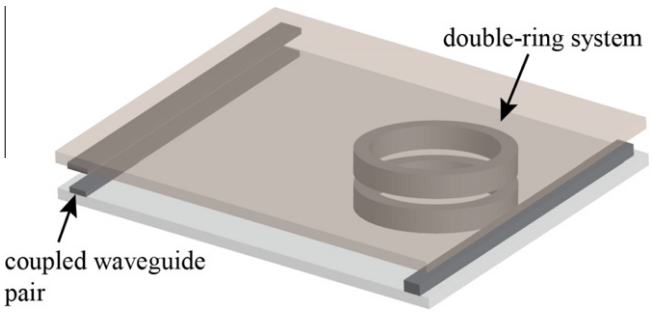

Fig. 8. Schematic design of a self-tuning resonator, adapted from Ref. [28].

The main challenge in demonstrating self-adaptive behavior is fabrication feasibility. The design of Ref. [28] requires two device layers. Each layer contains at least one waveguide and microring, and all devices within the layer must move together. Creative approaches and/or modified designs may be required to demonstrate self-adaptive concepts experimentally.

5.6. Slow light

Recent papers by Painter and coworkers have suggested the use of optomechanical effects to achieve slowing of light [74,75]. Motivated by the dramatic demonstration of stopped light in atomic gasses [76], resulting from electromagnetically-induced transparency (EIT), much recent work has attempted to demonstrate slow light in practical, on-chip microphotonic systems [77–79]. Applications of slow light, such as buffering and optical memories, are found in both classical and quantum information processing.

The maximum pulse delay that can be achieved in a slow light system is fundamentally limited by the lifetime of a "dark state," a resonance of the system that is weakly coupled to the outside world. The dark-state lifetime scales as the product of the resonance period times the quality factor. Painter and coworkers have suggested the use of a *mechanical* resonance as the dark state; the mechanical period is typically much longer than the optical period. In Ref. [74], the authors experimentally demonstrated a reflection spectrum characteristic of EIT in a optomechanical device. The structure is similar to Fig. 3b, however, the microcavity is formed by changing the hole size and shape near the center of the device, and the holes are elliptical rather than rectangular. At low temperature (8.7 K), an optically tunable delay of 50 ns with near-unity optical transparency was achieved. A method for tunable control of the optomechanical constant in time would further allow trapping and release of finite-bandwidth pulses.

5.7. Tunable lasers

The ability to tune the operating wavelength of a semiconductor laser by mechanically modifying the optical cavity is an intriguing application of optomechanical devices. Alegre et al. [80] have analyzed laser tuning in photonic crystal "zipper" cavities (similar to Fig. 3a). They propose to use two optical resonances, one corresponding to a master (or pump) frequency, and the other to the slave (or lasing) frequency. The optical force resulting from pump light would be used to adjust the separation between two nanobeams that make up the zipper. The change in separation will shift the frequency of the lasing mode. A particular advantage of the zipper structure is the ability to obtain large optomechanical coupling constants [80]; the shift in the lasing frequency scales as the product of the optomechanical coupling constants for the pump and lasing modes. However, wavelength-tunable lasers could also be realized through other microscale resonant photonic topologies with optomechanically adjustable air gaps. Tradeoffs between considerations such as output power, wavelength tunability, frequency stability, and mode profile will affect the choice of design.

6. Summary and comparison of device designs

In Table 1, we provide a comparison of selected experiments on optical forces in integrated photonic structures. For each experiment, we provide the mechanical resonance frequency of the device, the mechanical Q factor, the displacement obtained as well as the optical power used to do so, the optical Q factor, the optomechanical coupling constant, and the mechanical spring constant. We divide the experiments by device type. Several conclusions emerge from the table.

Table 1
Summary of selected experiments on optical forces in integrated photonic devices.

Device type	Device material	f_{mech} (MHz)	Q_{mech}	Displacement normalized to power (nm/mW)	Q_{opt}	$g_{OM}/2\pi$ (GHz/nm)	k (N/m)
Waveguides							
Single strip waveguide coupled with substrate [32]	Si + SiO_2	8.87	1850	2.5/1 (at mechanical resonance)	N/A	10*	3.6
Parallel strip waveguides [81]	Si	18.64	5400	2/3.2 (at mechanical resonance)	N/A	3*	16.8
Parallel strip waveguides [82]	Si	5.773	6000	Not given	N/A	3*	Not given
Microcavities							
Vertically-stacked wheels [33]	SiO_2	7 (22.5) **	Not given	17.7/1.7	10^6	31	9.25
Vertically-stacked wheels [34]	Si_3N_4	0.6 (8)**	2	20/3	10^4	8.8(+) 12.6(-)	1.2
Photonic-crystal cavities							
"Zipper" cavity [47]	Silicon nitride	8 (19) **	50–150	Not given	$\sim 10^4$–10^5	123	110
Nanobeam cavity [48]	Si	2250	1300	Not given	38,000	70*	Not given
Waveguide integrated with cavity							
Slot waveguide with reduced gap in cavity [24]	Si	760	500	Not given	60,000	200*	Not given
Guided resonance structures							
Double-layer photonic crystal [54]	InP	1.81	2	4/19.7	700(-)–1600(+)	43*	6.1

(+)/(−) Indicate values for attractive/repulsive modes.
* Indicates that the value was estimated from data provided in the reference.
** Values in parentheses indicate effective frequencies due to optical stiffening.

Waveguide devices offer the relative advantages of broadband operation and relative ease of fabrication. However, experiments have demonstrated relatively low optomechanical coupling strength (g_{OM}). The optomechanical coupling can be increased by integrating the waveguide with a cavity.

Microcavity devices (e.g. microrings, or "wheels"), exhibit relatively large displacements per unit of optical power compared to waveguide devices. However, photonic-crystal nanobeam microcavities offer much higher resonant frequencies (and hence, speed of operation), due to their reduced mass.

Guided-resonance devices allow for normal-incidence coupling from free space. However, the large mass of the structure corresponds to low mechanical resonance frequencies.

It is also important to note that the comparison between devices is not captured by these figures of merit alone; from the discussion in Sections 4 and 5 above, it should be apparent that the physical effects of optical forces that can be exploited in each device are different. We believe that a variety of device designs will find their niche in applications to on-chip optical signal manipulation.

7. Outlook and challenges

In summary, since the initial theoretical studies on optical forces between microphotonic devices, experimental progress has been rapid. New, creative ideas for exploiting optomechanical effects in highly tunable, on-chip devices are emerging daily.

Optomechanical effects offer the ability to tune devices by a much wider spectral range than other all-optical approaches, at the expense of relatively slow response speeds (typically several to hundreds of megahertz). In order to achieve high-speed, tunable optomechanical devices, efforts are needed to speed up the mechanical response. Proposals for obtaining GHz mechanical response speeds are of particular interest. The design of systems with large optomechanical coupling to higher-order mechanical resonances with large vibration frequencies are promising [46,83]. Using such strategies, it may be possible to build a GHz-rate all-optical modulator controlled by optical forces in the silicon-on-insulator platform.

To date, most experimental work has fabricated optomechanical devices in silicon, silicon nitride, and silicon oxide, materials with large Young's modulus. The displacement driven by optical force is usually on the order of 10's of nm, even in optical resonance-enhanced systems designed to have reduced mechanical stiffness [33,34]. To achieve larger displacements, and correspondingly larger tunability, it is of interest to explore the use of mechanically compliant materials, such as polymers, that can sustain a greater degree of deformation.

Lastly, the demonstration of optomechanical effects in integrated, on-chip systems containing multiple devices is a major goal. Careful design will be required to insure that the required optical power scales favorably with the number of devices. Schemes for optical power recycling will likely be required to enable on-chip all-optical positioning, tuning, and reconfiguration of complex photonic circuits.

Acknowledgment

The authors acknowledge funding from a National Science Foundation CAREER award under Grant No. 0846143.

References

[1] Ashkin A. History of optical trapping and manipulation of small-neutral particle, atoms, and molecules. IEEE J Selected Topics Quantum Electron 2000;6(6):841–56.
[2] Neuman KC, Block SM. Optical trapping. Rev Sci Instrum 2004;75(9):2787–809.
[3] Dorsel A et al. Optical bistability and mirror confinement induced by radiation pressure. Phys Rev Lett 1983;51(17):1550.
[4] Corbitt T et al. Squeezed-state source using radiation-pressure-induced rigidity. Phys Rev A 2006;73(2):023801.
[5] Vitali D et al. Macroscopic mechanical oscillators at the quantum limit through optomechanical cooling. J Opt Soc Am B 2003;20(5):1054–65.
[6] Povinelli ML et al. Evanescent-wave bonding between optical waveguides. Opt Lett 2005;30(22):3042–4.
[7] Noda S et al. Full three-dimensional photonic bandgap crystals at near-infrared wavelengths. Science 2000;289(5479):604–6.

[8] Almeida VR et al. All-optical control of light on a silicon chip. Nature 2004;431(7012):1081–4.
[9] Soref RA. Silicon-based optoelectronics. Proc IEEE 1993;81(12):1687–706.
[10] McNab S, Moll N, Vlasov Y. Ultra-low loss photonic integrated circuit with membrane-type photonic crystal waveguides. Opt Express 2003;11(22): 2927–39.
[11] Soref R. The past, present, and future of silicon photonics. IEEE J Selected Topics Quantum Electron 2006;12(6):1678–87.
[12] Pavesi L, Lockwood DJ. Silicon photonics. Topics in applied physics, vol. xvi. Berlin; New York: Springer; 2004.
[13] Haurylau M et al. On-chip optical interconnect roadmap: challenges and critical directions. IEEE J Selected Topics Quantum Electron 2006;12(6): 1699–705.
[14] Assefa S et al. CMOS-Integrated optical receivers for on-chip interconnects. IEEE J Selected Topics Quantum Electron 2010;16(5):1376–85.
[15] Xia F, Sekaric L, Vlasov Y. Ultracompact optical buffers on a silicon chip. Nat Photon 2007;1(1):65–71.
[16] Miller DAB. Rationale and challenges for optical interconnects to electronic chips. Proc IEEE 2000;88(6):728–49.
[17] Faraon A et al. Integrated quantum optical networks based on quantum dots and photonic crystals. New J Phys 2011;13:13.
[18] Joannopoulos JD, Meade RD, Winn JN. Photonic crystals: molding the flow of light, vol. ix. Berlin: Springer; 1995. 137p.
[19] Vahala K. Optical microcavities. Advanced series in applied physics, vol. xiii. Hackensack, NJ: World Scientific; 2004.
[20] Kippenberg TJ, Vahala KJ. Cavity opto-mechanics. Opt Express 2007;15(25): 17172–205.
[21] Favero I, Karrai K. Optomechanics of deformable optical cavities. Nat Photon 2009;3(4):201–5.
[22] Aspelmeyer M et al. Quantum optomechanics-throwing a glance [Invited]. J Opt Soc Am B. 2010;27(6):A189–97.
[23] Pernice WHP et al. Analysis of short range forces in opto-mechanical devices with a nanogap. Opt Express 2010;18(12):12615–21.
[24] Li M, Pernice WH, Tang HX. Ultrahigh-frequency nano-optomechanical resonators in slot waveguide ring cavities. Appl Phys Lett 2010;97(18): 183110.
[25] Mizrahi A, Schachter L. Mirror manipulation by attractive and repulsive forces of guided waves. Opt Express 2005;13(24):9804–11.
[26] Riboli F et al. Radiation induced force between two planar waveguides. The European Phys J D – Atomic, Molecular, Opt Plasma Phys 2008;46(1): 157–64.
[27] Povinelli ML et al. High-Q enhancement of attractive and repulsive optical forces between coupled whispering-gallery-mode resonators. Opt Express 2005;13(20):8286–95.
[28] Rakich PT et al. Trapping, corralling and spectral bonding of optical resonances through optically induced potentials. Nat Photon 2007;1(11):658–65.
[29] Taniyama H et al. Strong radiation force induced in two-dimensional photonic crystal slab cavities. Phys Rev B 2008;78(16):165129.
[30] Van Thourhout D, Roels J. Optomechanical device actuation through the optical gradient force. Nat Photon 2010;4(4):211–7.
[31] Pernice WHP, Li M, Tang HX. Theoretical investigation of the transverse optical force between a silicon nanowire waveguide and a substrate. Opt Express 2009;17(3):1806–16.
[32] Li M et al. Harnessing optical forces in integrated photonic circuits. Nature 2008;456(7221):480–4.
[33] Rosenberg J, Lin Q, Painter O. Static and dynamic wavelength routing via the gradient optical force. Nat Photon 2009;3(8):478–83.
[34] Wiederhecker GS et al. Controlling photonic structures using optical forces. Nature 2009;462(7273):633–6.
[35] Jackson JD. Classical electrodynamics, 3rd ed., vol. xxi. New York: Wiley; 1999. 808p.
[36] Povinelli ML et al. Slow-light enhancement of radiation pressure in an omnidirectional-reflector waveguide. Appl Phys Lett 2004;85(9):1466–8.
[37] Ng J et al. Strong optical force induced by morphology-dependent resonances. Opt Lett 2005;30(15):1956–8.
[38] Antonoyiannakis MI, Pendry JB. Electromagnetic forces in photonic crystals. Phys Rev B 1999;60(4):2363.
[39] Ma J, Povinelli ML. Mechanical Kerr nonlinearities due to bipolar optical forces between deformable silicon waveguides. Opt Express 2011;19(11):10102–10.
[40] Rakich PT, Popovic MA, Wang Z. General treatment of optical forces and potentials in mechanically variable photonic systems. Opt Express 2009;17(20):18116–35.
[41] Haus HA, Huang WP. Coupled-mode theory. Proc IEEE 1991;79(10):1505–18.
[42] Foresi JS et al. Photonic-bandgap microcavities in optical waveguides. Nature 1997;390(6656):143–5.
[43] Akahane Y et al. High-Q photonic nanocavity in a two-dimensional photonic crystal. Nature 2003;425(6961):944–7.
[44] Song BS et al. Ultra-high-Q photonic double-heterostructure nanocavity. Nature Mater 2005;4(3):207–10.
[45] Ryu HY, Notomi M, Lee YH. High-quality-factor and small-mode-volume hexapole modes in photonic-crystal-slab nanocavities. Appl Phys Lett 2003;83(21):4294–6.
[46] Chan J et al. Optical and mechanical design of a "zipper" photonic crystaloptomechanical cavity. Opt Express 2009;17(5):3802–17.
[47] Eichenfield M et al. A picogram- and nanometre-scale photonic-crystal optomechanical cavity. Nature 2009;459(7246):550–5.
[48] Eichenfield M et al. Optomechanical crystals. Nature 2009;462(7269):78–82.
[49] Notomi M et al. Optomechanical wavelength and energy conversion in high-Q double-layer cavities of photonic crystal slabs. Phys Rev Lett 2006;97(2):4.
[50] Fan S, Povinelli ML. Stopping light via dynamic tuning of coupled resonators. In: Slow light: science and applications. Boca Raton: CRC Press; 2009.
[51] Fan S et al. Slow and stopped light in coupled resonator systems. In: Photonic microresonator research and applications. Berlin/Heidelberg: Springer; 2010. p. 165–80.
[52] Fan S, Joannopoulos JD. Analysis of guided resonances in photonic crystal slabs. Phys Rev B 2002;65(23):235112.
[53] Liu V, Povinelli M, Fan SH. Resonance-enhanced optical forces between coupled photonic crystal slabs. Opt Express 2009;17(24):21897–909.
[54] Roh YG et al. Strong optomechanical interaction in a bilayer photonic crystal. Phys Rev B 2010;81(12):4.
[55] Rodriguez AW et al. Bonding, antibonding and tunable optical forces in asymmetric membranes. Opt Express 2010;19(3):2225–41.
[56] Rodriguez AW et al. Designing evanescent optical interactions to control the expression of Casimir forces in optomechanical structures. Appl Phys Lett 2011;98(19):3.
[57] Ma J, Povinelli ML. Effect of periodicity on optical forces between a one-dimensional periodic photonic crystal waveguide and an underlying substrate. Appl Phys Lett 2010;97(15):151102–3.
[58] Povinelli M, Johnson S, Joannopoulos J. Slow-light, band-edge waveguides for tunable time delays. Opt Express 2005;13(18):7145–59.
[59] Mutapcic A et al. Robust design of slow-light tapers in periodic waveguides. Eng Optim 2009;41(4):365–84.
[60] Johnson SG et al. Coupling, scattering, and perturbation theory: semi-analytical analyses of photonic-crystal waveguides. In: Proc 2003 5th international conference on transparent optical network; 2003.
[61] Hughes S et al. Extrinsic optical scattering loss in photonic crystal waveguides: role of fabrication disorder and photon group velocity. Phys Rev Lett 2005;94(3):033903.
[62] Johnson SG et al. Roughness losses and volume-current methods in photonic-crystal waveguides. Appl Phys B: Lasers Opt 2005;81(2):283–93.
[63] Maier SA. Plasmonics: fundamentals and applications, 1st ed., vol. xxiv. New York: Springer; 2007.
[64] Woolf D, Loncar M, Capasso F. The forces from coupled surface plasmon polaritons in planar waveguides. Opt Express 2009;17(22):19996–20011.
[65] Yang XD et al. Optical Forces in Hybrid Plasmonic Waveguides. Nano Letters 2011;11(2):321–8.
[66] Huang CG, Zhu L. Enhanced optical forces in 2D hybrid and plasmonic waveguides. Opt Lett 2010;35(10):1563–5.
[67] Pernice WHP, Li M, Tang HX. A mechanical Kerr effect in deformable photonic media. Appl Phys Lett 2009;95(12):123503–7.
[68] Ma J, Povinelli ML. Large tuning of birefringence in two strip silicon waveguides via optomechanical motion. Opt Express 2009;17(20):17818–28.
[69] Saleh BEA, Teich MC. Fundamentals of photonics 1991.
[70] Fong KY et al. Tunable optical coupler controlled by optical gradient forces. Opt Express 2011;19(16):15098–108.
[71] Eichenfield M et al. Actuation of micro-optomechanical systems via cavity-enhanced optical dipole forces. Nat Photon 2007;1(7):416–22.
[72] Wiederhecker GS et al. Broadband tuning of optomechanical cavities. Opt Express 2011;19(3):2782–90.
[73] Popovic MA, Rakich PT. Optonanomechanical self-adaptive photonic devices based on light forces: a path to robust high-index-contrast nanophotonic circuits. In: Eldada LA, Lee EH, editors. Optoelectronic integrated circuits XI. Bellingham: SPIE-Int Soc Optical Engineering; 2009.
[74] Safavi-Naeini AH et al. Electromagnetically induced transparency and slow light with optomechanics. Nature 2011;472(7341):69–73.
[75] Chang DE et al. Slowing and stopping light using an optomechanical crystal array. New J Phys 2010;13:26.
[76] Harris SE. Electromagnetically induced transparency. Phys Today 1997;50(7): 36–42.
[77] Yanik MF et al. Stopping light in a waveguide with an all-optical analog of electromagnetically induced transparency. Phys Rev Lett 2004;93(23):4.
[78] Yanik MF, Fan SH. Stopping and storing light coherently. Phys Rev A 2005;71(1):10.
[79] Fan SH et al. Advances in theory of photonic crystals. J Lightwave Technol 2006;24(12):4493–501.
[80] Alegre TPM, Perahia R, Painter O. Optomechanical zipper cavity lasers: theoretical analysis of tuning range and stability. Opt Express 2010;18(8): 7872–85.
[81] Li M, Pernice WHP, Tang HX. Tunable bipolar optical interactions between guided lightwaves. Nat Photon 2009;3(8):464–8.
[82] Roels J et al. Tunable optical forces between nanophotonic waveguides. Nat Nano 2009;4(8):510–3.
[83] Gavartin E et al. Optomechanical coupling in a two-dimensional photonic crystal defect cavity. Phys Rev Lett 2011;106(20):203902.